

RESEARCH

Open Access



“Just right” combinations of adjuvants with nanoscale carriers activate aged dendritic cells without overt inflammation

Ananya Ananya^{1,2}, Kaitlyn G. Holden¹, Zhiling Gu³, Dan Nettleton³, Surya K. Mallapragada^{1,2}, Michael J. Wannemuehler¹, Marian L. Kohut^{1,4} and Balaji Narasimhan^{1,2*}

Abstract

Background The loss in age-related immunological markers, known as immunosenescence, is caused by a combination of factors, one of which is inflammaging. Inflammaging is associated with the continuous basal generation of proinflammatory cytokines. Studies have demonstrated that inflammaging reduces the effectiveness of vaccines. Strategies aimed at modifying baseline inflammation are being developed to improve vaccination responses in older adults. Dendritic cells have attracted attention as an age-specific target because of their significance in immunization as antigen presenting cells that stimulate T lymphocytes.

Results In this study, bone marrow derived dendritic cells (BMDCs) were generated from aged mice and used to investigate the effects of combinations of adjuvants, including Toll-like receptor, NOD2, and STING agonists with polyanhydride nanoparticles and pentablock copolymer micelles under in vitro conditions. Cellular stimulation was characterized via expression of costimulatory molecules, T cell-activating cytokines, proinflammatory cytokines, and chemokines. Our results indicate that multiple TLR agonists substantially increase costimulatory molecule expression and cytokines associated with T cell activation and inflammation in culture. In contrast, NOD2 and STING agonists had only a moderate effect on BMDC activation, while nanoparticles and micelles had no effect by themselves. However, when nanoparticles and micelles were combined with a TLR9 agonist, a reduction in the production of proinflammatory cytokines was observed while maintaining increased production of T cell activating cytokines and enhancing cell surface marker expression. Additionally, combining nanoparticles and micelles with a STING agonist resulted in a synergistic impact on the upregulation of costimulatory molecules and an increase in cytokine secretion from BMDCs linked with T cell activation without excessive secretion of proinflammatory cytokines.

Conclusions These studies provide new insights into rational adjuvant selection for vaccines for older adults. Combining appropriate adjuvants with nanoparticles and micelles may lead to balanced immune activation characterized by low inflammation, setting the stage for designing next generation vaccines that can induce mucosal immunity in older adults.

Keywords Immunosenescence, Inflammation, Dendritic cells, Vaccines, Pattern recognition receptors, Nanoparticles, Micelles, Cytokines, Principal component analysis

*Correspondence:

Balaji Narasimhan
nbalajj@iastate.edu

Full list of author information is available at the end of the article



© The Author(s) 2023. **Open Access** This article is licensed under a Creative Commons Attribution 4.0 International License, which permits use, sharing, adaptation, distribution and reproduction in any medium or format, as long as you give appropriate credit to the original author(s) and the source, provide a link to the Creative Commons licence, and indicate if changes were made. The images or other third party material in this article are included in the article's Creative Commons licence, unless indicated otherwise in a credit line to the material. If material is not included in the article's Creative Commons licence and your intended use is not permitted by statutory regulation or exceeds the permitted use, you will need to obtain permission directly from the copyright holder. To view a copy of this licence, visit <http://creativecommons.org/licenses/by/4.0/>. The Creative Commons Public Domain Dedication waiver (<http://creativecommons.org/publicdomain/zero/1.0/>) applies to the data made available in this article, unless otherwise stated in a credit line to the data.

Background

Immunosenescence is a process of immune system dysfunction associated with aging. It is a complex phenomenon that can have major impacts on both innate and adaptive immunity, influencing chronic illnesses [1–3]. Immunosenescence is associated with a diminishing capacity to mount an effective immune response and the senescence of immune cells [4]. This cellular senescence is a hallmark of aging, wherein cells cease to divide and undergo an irreversible cessation of replication [4, 5]. The senescence-associated secretory phenotype (SASP) of senescent cells is characterized by the release of proinflammatory cytokines and matrix-degrading molecules. Disproportionate production of stimulating mediators like cytokines, chemokines, and acute phase reactants, as seen with SASP, often leads to a persistent, systemic, low-grade inflammatory condition known as “inflammaging” [6–8]. Inflammaging is multifactorial, driven to some extent by damaged organelles, reduction of autophagy, increased danger/damage-associated molecular pattern (DAMPs) [8] that contribute to chronic stimulation of the innate immune system [7] which is followed by a rise in senescent cell accumulation, and the production of proinflammatory cytokines [9–12]. It has been demonstrated that greater levels of inflammatory cytokines secreted by immune cells is associated with poor vaccination response [13, 14]. Some studies have also shown that preexisting inflammation could lead to poor vaccine efficacy in multiple vulnerable populations (e.g., older adults, people with autoimmune disorders) that may most critically need vaccination [14–17].

Dendritic cells (DCs) are a heterogeneous collection of antigen-presenting cells (APC) that play a crucial role in vaccination because they prime T cell immune responses against antigens via a peptide-MHC interaction (Signal 1) [18]. When triggered by microbial-associated molecular patterns (MAMPs) via the interaction with pattern recognition receptors (PRRs) such as Toll-like receptors (TLRs) [19, 20], intracytoplasmic NOD-like receptors (NLRs) [21, 22] and C-type lectin receptors (CLRs) [23, 24], DCs upregulate costimulatory molecule expression (Signal 2) and produce cytokines (Signal 3) that contribute to T cell activation [25]. The extent of DC costimulatory molecule expression and cytokine profile shape T cell activation and memory [26]. However, the function of DCs in linking innate and adaptive immune response in older adults is not well understood [27]. It has been shown that with aging, DCs are less effective in processing and presenting antigens to T cells [28–31] and their cytokine output is not optimal for stimulating potent adaptive immune responses [32, 33]. Therefore, to optimize vaccine design for older adults, it would be useful to identify strategies aimed at enhancing the functionality of

DCs [32]. Vaccines that are directed towards DC stimulation provide a wealth of options for modulating humoral immune responses, including fine-tuning T cell polarization and managing antigen accessibility for B cells [34]. Adjuvants (e.g., biomaterials, synthetic materials, viral vectors) are immunostimulants that are added to vaccines to increase and improve the amplitude and duration of the immunological response. Adjuvants initiate effector functions of APCs by inducing an inflammatory profile [35, 36]. Immunosenescence and the age-related rise in the proinflammatory state may increase susceptibility to infection and reduce vaccine responsiveness. Effects of inflammaging are present within tissues including the lung, which must be taken into account in the development of vaccines for mucosal sites [37]. Therefore, vaccines targeted at enhancing the aged immune system must simultaneously seek to mitigate the inflammatory state and optimize adaptive immunity [38]. It is possible that suppressing or modifying inflammation, as opposed to eliminating it, might provide a unique opportunity to induce potent immune responses in aged populations. To improve vaccine-induced immunity, it would be beneficial to create new “combination vaccines” that can either broadly or selectively balance and/or channel certain basal inflammation pathways [35].

Effective stimulants are needed to counteract the low-grade inflammatory state that may impede vaccination responses, as well as to improve innate and adaptive immune responses to vaccines and to provide long term protection against infection in aged individuals [39–41]. To improve immunogenicity in older adults, polymeric adjuvants may be modified to include immunomodulatory drugs [42], and polymer chemistry can be tailored to regulate protein release kinetics [43]. In this context and to combat age-related deficits in vaccination response, we have created two effective and safe vaccine delivery systems based on biodegradable polyanhydride nanoparticles composed of 1,8-bis(*p*-carboxyphenoxy)-3,6-dioxaoctane (CPTEG) and 1,6-bis (*p*-carboxyphenoxy) hexane (CPH) [44–46] and self-assembling nanoscale amphiphilic poly(diethyl aminoethyl methacrylate) (PDEAEM)-Pluronic pentablock copolymer (PBC) micelles [46]. Both platforms induce ‘optimal’ inflammation, and from the perspective of aging, are complementary based on the observations that nanoparticles enhance T cell immunity [47] and micelles boost B cell responsiveness [48]. We have shown that PBC micelles and nanoparticles, unlike TLR ligands, induce much less secretion of inflammatory cytokines by DCs [49]. Nanovaccines can be designed by judiciously combining adjuvants and antigens with nanoparticles and micelles. In comparison to traditional vaccine adjuvants, such as alum, nanovaccines offer significant benefits, including

improved thermal stability, decreased reactogenicity, and increased shelf-life stability of the payload [50]. The polyanhydride-based Gliadel[®] wafer has been approved for use in humans [51], and we have shown that polyanhydride nanoparticles have excellent tissue compatibility in mice [52]. Additionally, there is no indication of toxicity, inflammation, or necrosis at the injection site when using PBC micelles in mice [53]. At body temperature (37 °C), high concentrations of polymer micelles in aqueous solution produce physical gels that entrap proteins and allow for long-term antigen delivery [54–57]. Amphiphilic regions improve cellular uptake [58, 59], while the Pluronic block encourages endocytosis [60]. PDEAEM has also been shown to enhance adjuvanticity [61, 62].

In this study, we tested several PRR-dependent adjuvants together with our two polymeric “adjuvant nanocarriers” (i.e., 20:80 CPTEG:CPH nanoparticles (NPs) and PBC micelles (Mi)) as a means of activating aged bone marrow derived DCs (BMDCs). The rationale for the choice of these adjuvants and the types of immune

responses induced by them are outlined in Table 1. Because each PRR adjuvant can impact different mechanisms, compensating for the impaired innate and adaptive immunity of older adults, their targeted usage, either alone or in combination, will likely be vital in future vaccine development [27]. Our objective was to identify adjuvant/biomaterial combination(s) that appropriately stimulate aged BMDCs by elevating costimulatory molecule expression (CD40, CD80, CD86) and inducing cytokines (IL-12p70, IFN α , IL-6, IFN β , IFN γ) associated with T cell activation (CD4⁺ T_{fh} and CD8⁺ memory) while promoting “optimal” inflammation without excessive production of IL-1 β , IL-6, TNF α , and IL-12p40.

Results

Upregulation of costimulatory molecule expression by adjuvants

As an assessment of BMDC maturation through upregulation of costimulatory molecule expression, we investigated the stimulatory effect of several agonists

Table 1 Experimental stimulants, their immunological function, and dosage used

	Immune stimulant	Agonist	Immune response	Dosage
1	Class B CpG oligonucleotide	TLR9 agonist	Promotes activation and maturation of plasmacytoid DCs (pDCs) and stimulate small amount of INF α and IFN β [63] Strongly activates B cells [64, 65] Induces secretion of IL-6, IL-10, IL-12 [66]	5 μ g/mL
2	Bis-(3'-5')-cyclic dimeric guanosine monophosphate (c-di-GMP) (CDN)	STING Agonist	Increases production of IL-12, IFN- γ , IL-8, MCP-1, and RANTES Enhances T cell stimulatory activity [67]	1 μ g/mL
3	Flagellin from <i>B. subtilis</i> (FLA-BS)	TLR5 [68], NLRs, NLRC4 and NAIP5 [69]	Extracellular FLA-BS activation through TLR5 triggers MyD88- dependent- B activation, cytokine, and NO generation [70]. Detection of intracellular flagellin by NLRC4 and NAIP5 results in the formation of an inflammasome, which activates caspase-1 of IL-1 β and IL-18 [71, 72].	100 ng/mL
4	Lipopolysaccharides (LPSs)	TLR2 and TLR4	Powerful T cell adjuvant that promotes clonal expansion of B cells, resistance to growth factor deprivation, and Th cell differentiation of activated T cells. Induces production of interleukin-1 β (IL-1 β), IL-6, IL-10, IL-12, and TNF α [73]	1 μ g/mL
5	Monophosphoryl-Lipid A (MPLA)	TLR 4	Induces a strong Th1 response Promotes IFN- γ production by Ag- specific CD4 T cells [74] Enhance production of antigen-specific CD8 cytotoxic T lymphocytes [75] Induces production of IL-1 β , IL-10, IL-6, IL-8, and TNF- α [73]	1 μ g/mL
6	Muramyl dipeptide (MDP)	NOD2	MDP increases the production of IL-10 when coupled with TLR2 agonists [76] MDP's potential stimulation of NLRP3 and NLRP1 produces IL-1 β [77] Combining MDP with LTA (a TLR2 agonist) stimulates human monocyte derived DCs and increases TNF- α and IL-12 secretion [78]	1 μ g/mL
7	R848	TLR7 and TLR 8	R848 strongly induces cytokines such as TNF- α , IFN α , IL-12, and IFN- γ Helps in the induction of Th1 and Th2 cell types [79].	100 ng/mL
8	Polyanhydride NP	–	NP are readily phagocytosed by DCs, allow sustained release of antigen, and show a safe toxicological profile [80, 81] Induce T cell responses Has been shown to cause low inflammation [49]	100 μ g/mL
9	PBC Micelles	–	Micelles offer pH-responsive micellization and gelation to aid the antigen endosomal escape in a sustainable manner Induce B cell responses Has been shown to cause low inflammation [82]	12.5 mg/mL

on BMDCs generated from aged mice. BMDCs were gated based on FSC-A and SSC-A and doublets were excluded (Fig. 1a). Live (zombie NIR negative) cells were then selected, followed by selecting BMDCs that were positive for CD11c expression (Fig. 1a). As a representative example, histograms depicting the elevation of the cell surface markers CD40, CD80, and CD86 in NP+Mi+CpG-treated cells compared to untreated cells are shown in Fig. 1b. Immune stimulants, as single adjuvants and in combination with biomaterial carriers, differentially affected the expression of costimulatory molecules. To differentially evaluate these effects, we used a mixed linear model (described in Section 4.6), and in the results that follow, we denote adjusted *p*-values as *q*-values to indicate the degree of statistical significance. In comparison to unstimulated cells, treating the cells with CpG, LPS, MPLA, NP+Mi+CpG, NP+Mi+CDN, or NP+Mi+R848 increased the surface expression of all costimulatory molecules measured (i.e., CD40, CD80, and CD86; Fig. 1c; $q < 0.001$). In contrast, CDN upregulated only CD40 ($q < 0.001$), MDP upregulated CD40 ($q < 0.001$) and CD80 ($q < 0.01$), and FLA-BS upregulated CD40 ($q < 0.05$) and CD80 ($q < 0.05$). Moreover, cells treated with NP and Mi did not differ significantly from untreated controls in terms of their cell surface expression (Fig. 1c). “Dual” combinations of CDN and CpG with either NP or Mi were also included as treatment groups (see supplement, Fig. S1), but because these combinations did not outperform either single adjuvant or triple combinations, they are not discussed further in the main manuscript.

Cytokine and chemokine secretion

In order to more clearly present the findings from a large panel, the cytokines were categorized as: (i) cytokines associated with T cell activation (IL-12p70, IFN α , IL-6, IFN γ , IFN β); (ii) proinflammatory cytokines (IL-1 β , IL-1 α , IL-6, TNF α , IL-12p40); and (iii) cytokines with regulatory effects on DCs (IL-10). We assessed levels of cytokines and chemokines from supernatants of aged BMDCS stimulated for 24 h with various stimulants and dual/triple combinations as mentioned previously.

Cytokines associated with T cell activation

When compared to untreated cells, cells treated with NP+Mi+R848, LPS, R848, CpG, MPLA, and NP+Mi+CpG significantly increased IL-12p70 production ($q < 0.001$). CDN also increased IL-12p70 secretion ($q < 0.05$). We observed no significant impact of NP+Mi+CDN, NP, MDP, FLA-BS, or Mi on IL-12p70 production. NP+Mi+R848, LPS, R848, CpG, MPLA, and NP+Mi+CpG increased IFN γ ($q < 0.001$). However, NP+Mi+CDN, NP, MDP, FLA-BS, CDN, and Mi had no detectable effect on IFN γ . All stimulants generated considerable levels of IL-6 compared to untreated cells ($q < 0.001$ for all treatments except CDN $q < 0.05$) (Fig. 2). We also measured an expanded panel of T cell activating cytokines in a subset of cells that included IFN β and IFN α (Sup. Figure 2b). IFN β was strongly induced by LPS ($q < 0.001$), CpG ($q < 0.001$), MPLA ($q < 0.001$), NP+Mi+CpG ($q < 0.001$), NP+Mi+CDN ($q < 0.001$) and NP+Mi+R848 ($q < 0.01$). We observed no impact of NP, MDP, R848, and CDN on IFN β production. However, FLA-BS and Mi appeared to downregulate IFN β but there is no statistical evidence suggesting the downward regulation is significant. In addition, LPS, CpG, MPLA, NP+Mi+CpG, NP+Mi+CDN, and CDN strongly increased the production of IFN α ($q < 0.001$). R848 ($q < 0.01$) and NP+Mi+R848 ($q < 0.05$) also increased IFN α production relative to untreated cells. We observed no significant impact of NP, MDP, FLA-BS, and Mi on IFN α production.

Proinflammatory cytokines

NP+Mi+R848, LPS, R848, CpG, MPLA, NP+Mi+CpG, and NP+Mi+CDN and NP increased IL-1 β production ($q < 0.001$). FLA-BS also upregulated IL-1 β production, though not as strongly ($q < 0.05$). MDP, CDN, and Mi had no effect on IL-1 β production. TNF α was produced in large quantities by cells treated with NP+Mi+R848, LPS, R848, CpG, MPLA, NP+Mi+CpG, and NP+Mi+CDN and Mi ($q < 0.001$). TNF α production was likewise increased by NP treatment ($q < 0.05$). MDP, FLA-BS, and CDN had no effect on TNF α production compared to untreated cells. LPS, R848, CpG, MPLA, NP+Mi+CpG, and NP+Mi+R848 promoted the production of IL-12p40 ($q < 0.001$). NP+Mi+CDN and MDP both increased IL-12p40

(See figure on next page.)

Fig. 1 **a** Gating strategy used in flow cytometric analyses to gate the cells of interest after surface staining. **b** Representative histogram plot for unstimulated (pink) vs NP+Mi+CpG (blue) for the upregulation of costimulatory molecules CD40, CD80, and CD86 on CD11c+ bone marrow-derived dendritic cells from aged mice. **c** Estimates of \log_2 fold change (\log_2FC) and regulation tests for costimulatory molecules expressed on cell surfaces after stimulation by various adjuvants. All treatments were applied to cells from each of six mice ($n = 6$) with up to three technical replicates. The horizontal axis represents adjuvants; the vertical axis represents responses; color scale represents the \log_2FC ; asterisks represent the degree of significance: **** $q < 0.001$, *** $q < 0.01$, ** $q < 0.05$. Dual adjuvant combinations are omitted from the main text for conciseness. Please refer to Supplementary Fig. S1 for results of dual adjuvants and controls

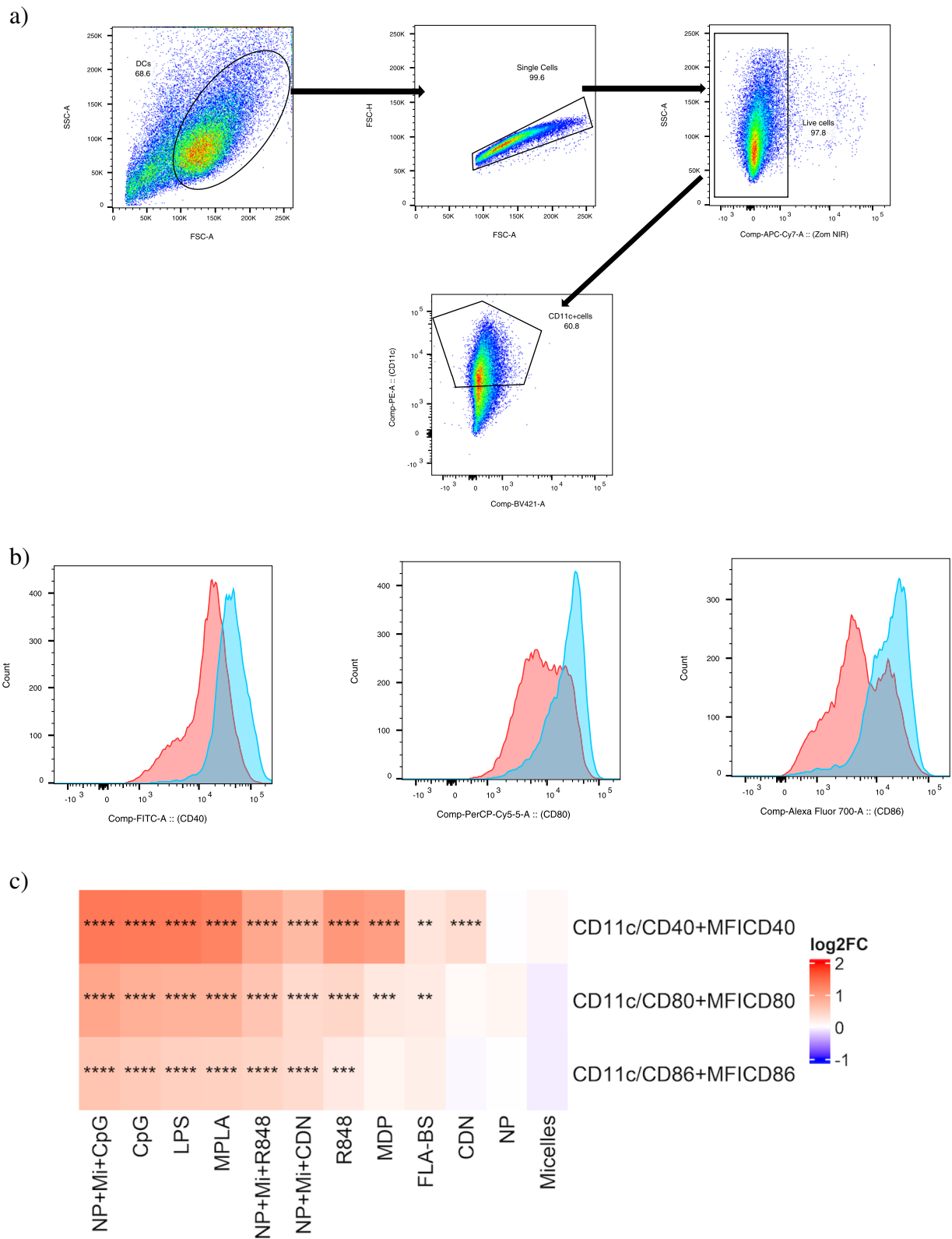


Fig. 1 (See legend on previous page.)

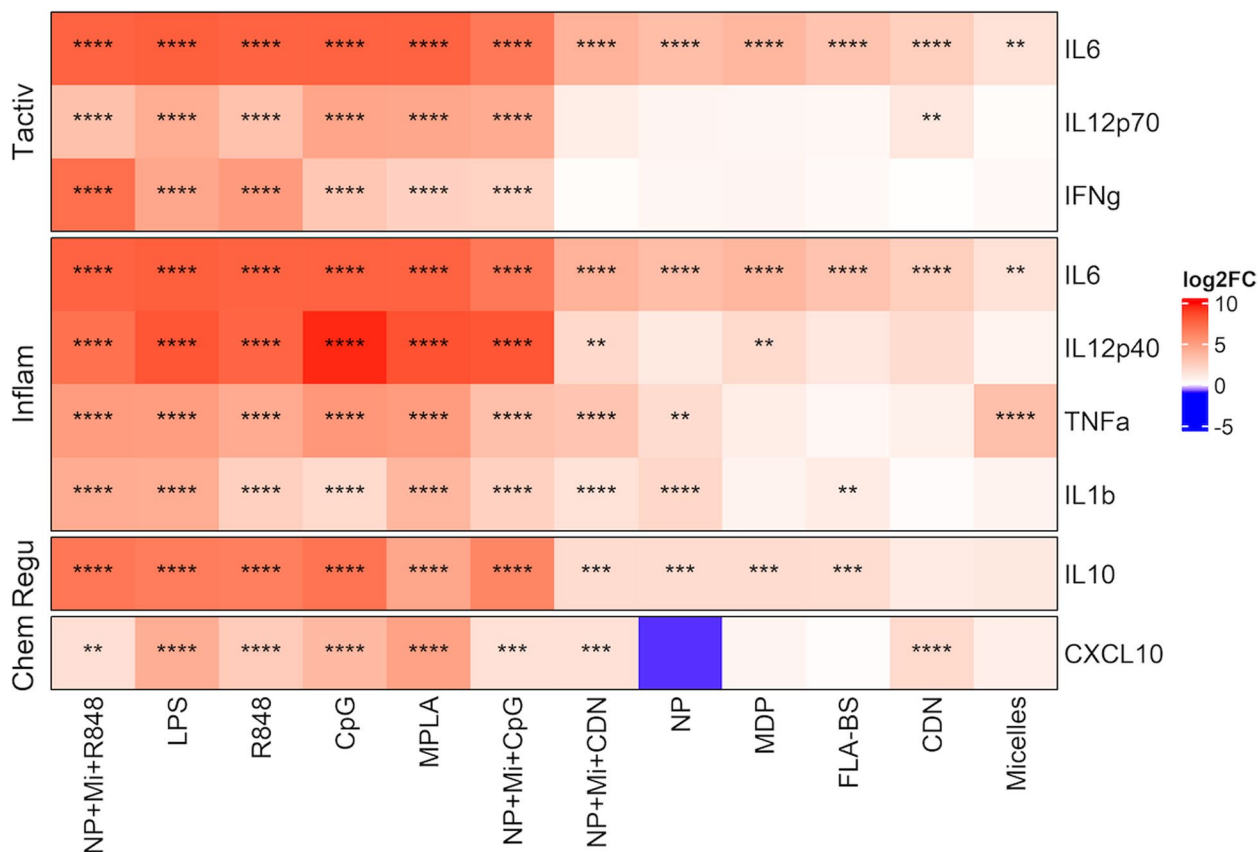


Fig. 2 Estimates of \log_2 fold change (\log_2FC) and tests of regulation from mixed linear model analysis of cytokines produced by BMDCs generated from aged mice. Stimulants shown here include single adjuvants and their related triple combination. Each treatment was replicated with supernatants collected from cultures of cells from each of 3-6 animals. Results for dual adjuvants and their controls are shown in Supplementary Fig. S2a and chemokines are shown in Supplementary Fig. S2b

secretion ($q < 0.05$). However, NP, FLA-Bs, CDN, and Mi had no effect on IL-12p40 production (Fig. 2). LPS, CpG, and R848 increased IL-1 α production ($q < 0.05$), while NP+Mi+CDN inhibited IL-1 α expression. MPLA, NP+Mi+R848, NP+Mi+CpG, NP, MDP, FLA-BS, Mi, and CDN did not stimulate IL-1 α production (Fig. S2b).

Regulatory cytokines

NP+Mi+R848, LPS, R848, CpG, MPLA, NP+Mi+CpG, and NP+Mi+CDN increased IL-10 production ($q < 0.001$). NP+Mi+CDN, NP, MDP, and FLA-BS also increased IL-10 production ($q < 0.01$), though less strongly. There was no effect of Mi and CDN on IL-10 production (Fig. 2). Only Mi increased the production of CCL2 ($q < 0.05$) while CpG downregulated the production of CCL2 (Fig. S2b).

Chemokines

LPS, R848, CpG, MPLA, and CDN treatment enhanced CXCL10 levels compared to untreated cells ($q < 0.001$). CXCL10 production was also increased

by NP+Mi+CpG, NP+Mi+CDN ($q < 0.01$), and NP+Mi+R848 ($q < 0.05$) stimulation. We did not observe any impact of Mi, MDP, or FLA-BS on the production of CXCL10. However, CXCL10 was downregulated by NP (Fig. 2). An expanded panel of chemokines was also assessed on a subset of cells (Sup. Figure 2b). Dual treatments (i.e., NP+CpG, Mi+CpG, NP+CDN and Mi+CDN) were also evaluated, but none of these combinations were superior to single adjuvant or triple combinations (Fig. S2a).

Principal Component Analysis (PCA)

To facilitate the clustering of the adjuvants' effects compared to unstimulated cells, we performed PCA for costimulatory molecules and cytokines separately. All responses were log-transformed ($\log(Y+1)$) and standardized. The biplots in Fig. 3a and b show arrows (loading plot) that represent responses to treatment. The direction of the arrows shows how much weight each response has on the first two principal components (PCs). Each point on the PCA plot represents the response of BMDCs from

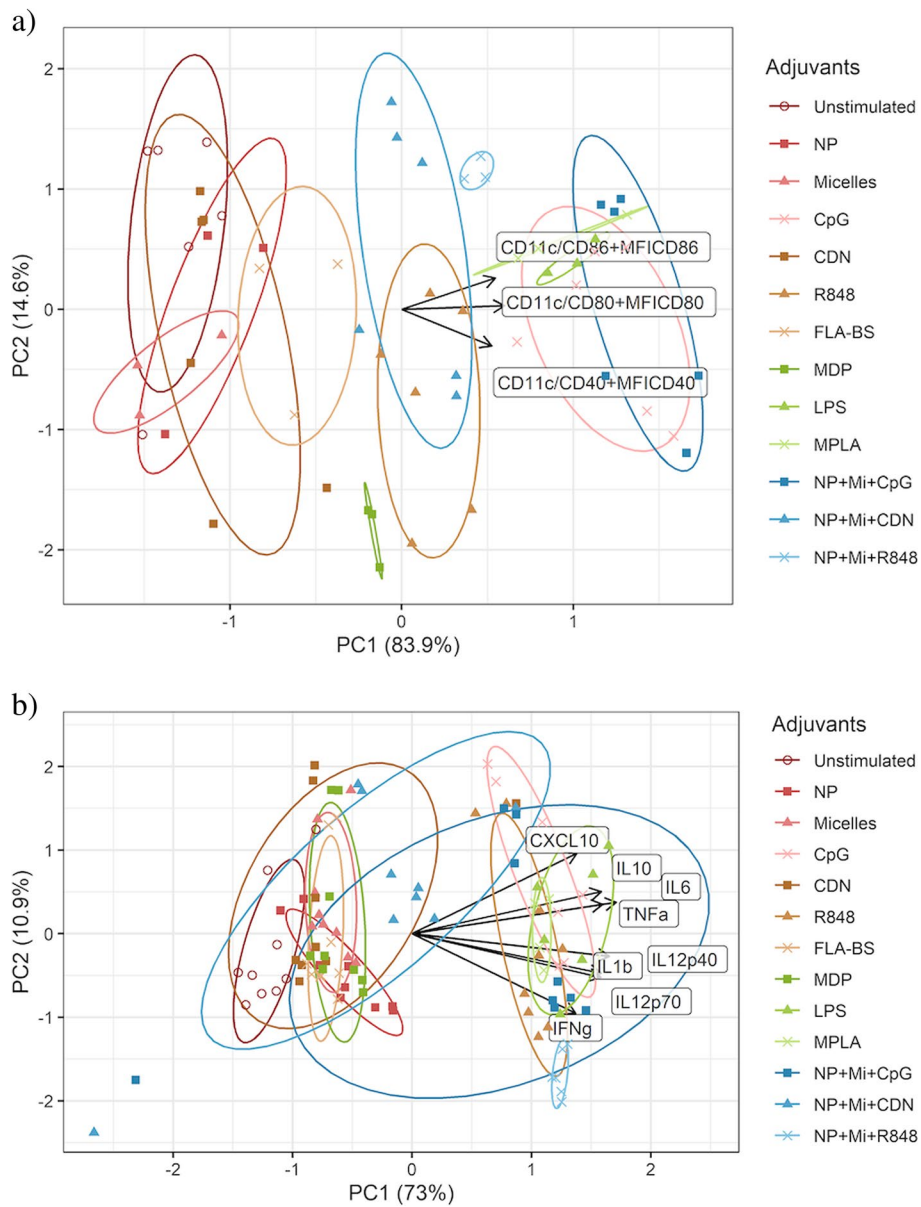


Fig. 3 **a** PCA analysis of costimulatory molecule expression for the combined datasets of all experiments. Dual adjuvant groups are omitted in this analysis. The response names near arrows represents abbreviations as follows. The responses are *Cd11c + Cd86+*, *CD11c + CD80+*, and *CD11c + CD40+* from top to bottom. The lengths of the arrows in this figure were scaled down for readability. **b** PCA analysis of cytokines for the combined datasets of all experiments. Dual adjuvants are omitted in this analysis. The responses are CXCL10, IL10, IL6, TNF α , IL12p40, IL1b, IL12p70, IFN γ from top to bottom

a single aged mouse to a single adjuvant or adjuvant-biomaterial combination. The points are colored to represent different adjuvants and their combinations, and their location is determined by their first two PC scores, where similarities are present with respect to location for points corresponding to the same adjuvant. Finally, the biplot (loading plot + PCA plot) shows how one adjuvant affects responses compared to that of unstimulated

cells by examining the projected distance and direction between the corresponding ellipse covering most points corresponding to the adjuvant and the ellipse covering most points for the unstimulated cells.

Figure 3a shows that the points representing cells stimulated by NP + Mi + CpG, CpG, LPS, MPLA, and NP + Mi + R848 are to the right of the unstimulated points, indicating that they contribute to the increase in

Table 2 Differences in PC scores and Euclidean distance (in the space defined by PC1 and PC2) between treatments and control (untreated cells) for costimulatory molecule expression. We observe a cluster of adjuvants (MPLA, LPS, CpG, and NP + Mi + CpG) that suggest greater upregulation of costimulatory molecule expression than the other adjuvants

Adjuvants	PC1(Adjuv)-PC1(Media)	PC2(Adjuv)-PC2(Media)	Distance(PC1,PC2)
NP	0.32	-0.45	0.55
CDN	0.42	-0.61	0.74
Micelles	-0.1	-0.82	0.82
FLA-BS	1.1	-0.51	1.21
NP + Mi + CDN	2.18	-0.15	2.19
MDP	1.81	-1.69	2.47
R848	2.32	-0.97	2.52
NP + Mi + R848	2.76	0.29	2.78
MPLA	3.54	-0.09	3.54
LPS	3.65	-0.19	3.66
CpG	3.95	-0.58	4.00
NP + Mi + CpG	4.25	-0.44	4.27

Table 3 PC score differences and Euclidean distance (in the space defined by PCs 1 and 2) between treatments and control (untreated cells) for cytokine production. We observe a cluster of adjuvants (NP + Mi + CpG, R848, MPLA, CpG, LPS, and NP + R848 + Mi) that may lead to greater cytokine production than other adjuvants

Adjuvants	PC1(Adjuv)-PC1(Media)	PC2(Adjuv)-PC2(Media)	Distance(PC1,PC2)
FLA-BS	1.15	0.14	1.16
Micelles	1.25	0.54	1.37
MDP	1.39	0.32	1.42
CDN	1.3	0.62	1.44
NP	1.53	-0.24	1.55
NP + Mi + CDN	2.16	0.68	2.27
NP + Mi + CpG	4.66	0	4.66
R848	5.27	0.07	5.27
MPLA	5.52	0.24	5.53
CpG	5.51	0.89	5.59
NP + Mi + R848	5.89	-1.37	6.05
LPS	6.11	0.34	6.12

responses in the direction of the first PC when compared to unstimulated cells. The horizontal projection of the arrows shows that the first PC is composed of a nearly equal-weighted sum of all three responses (i.e., CD80, CD86, and CD40 expression). Similarly, LPS, MPLA, CpG, R848 NP + Mi + R848 and NP + Mi + CDN are also observed to the right of the unstimulated cells in Fig. 3b.

We calculated the differences in PC scores between the various adjuvants and the control. We observed a potential cluster of MPLA, LPS, CpG, and NP + Mi + CpG that increase costimulatory expression compared to other adjuvants (Table 2 and Fig. S3). In terms of cytokines, we identified a cluster of NP + Mi + CpG, R848, MPLA, CpG, LPS, and NP + R848 + Mi (Table 3 and Fig. S4). Finally, we performed a second PCA analysis for the cytokines categorized as either T cell activating (Fig. 4) or proinflammatory (Fig. 5). For the former, a cluster of NP + Mi + CpG, R848, NP + Mi + R848, CpG, MPLA, and LPS was identified that produced cytokines linked with T cell activation (Table 4 and Fig. S5). For the latter, a potential cluster of NP + Mi + CpG, MPLA, CpG, NP + Mi + R848, and LPS was identified, with R848 being the most proinflammatory (Table 5 and Fig. S6).

Discussion

Aging is associated with impaired immunological function and a higher risk of infection [83]. Although vaccination is a tried-and-true method of preventing infections in older adults, it has been shown that the initial antibody response to vaccination declines with age and that older persons have a shorter immunization duration [84–86], and that pre-existing inflammation leads to poor antigen presentation [15]. The poor responsiveness of the aging immune system may be addressed by increasing both the innate and adaptive immunological responses to vaccination and by counteracting the low-grade inflammatory state that could otherwise impede vaccine responses in older persons [40].

DCs are potential targets to improve immunity because of their shorter life spans and their location upstream of the activation of T and B lymphocytes [18, 26, 87]. Recent years have seen growing evidence supporting the role of DC function in immunological disorders, and promising research into targeting DCs for treating several diseases [88]. Adjuvants have an important role in increasing the humoral and cellular immune responses elicited by vaccines by triggering local proinflammatory cytokine production, activating innate immune cells, and stimulating antigen presentation [89]. However, when administered by themselves, many of them display adverse effects such as overt inflammation [90]. Our studies show that optimal stimulation of aged BMDCs may be achieved by combining adjuvants with our polymeric adjuvant nanocarriers without exacerbating inflammation. Through a multi-faceted approach of assessing costimulatory expression and cytokine production, we determined which combination nanovaccines were most effective at stimulating APC generated from aged mice and minimizing induction of pro-inflammatory cytokine responses.

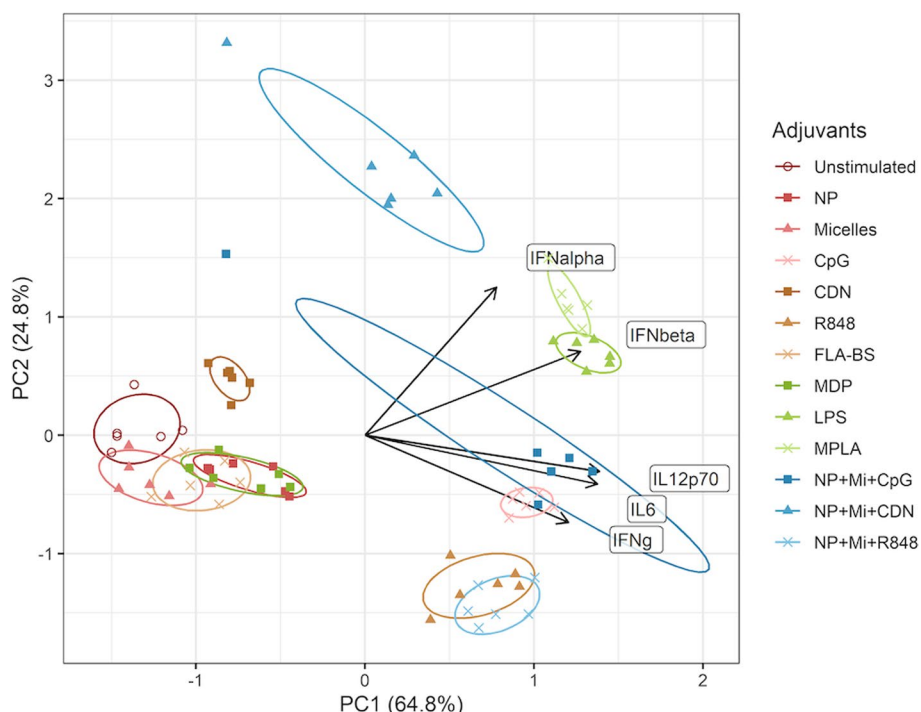


Fig. 4 PCA for cytokines associated with T cell activation ($CD4^+$ Tfh and $CD8^+$ memory). The responses are IFN α , IFN β , IL-6, IL-12p70, and IFN γ from top to bottom

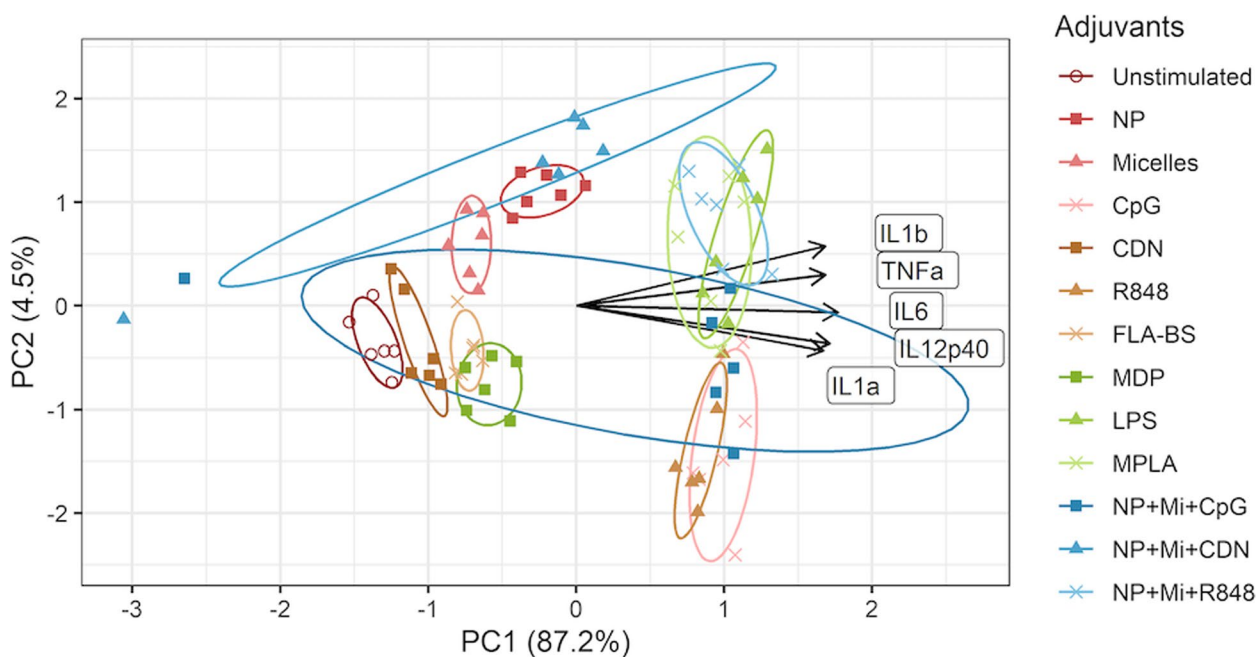


Fig. 5 PCA for proinflammatory cytokine secretion. The responses are IL-1 β , TNF α , IL-6, IL-12p40, and IL-1 α from top to bottom

Our results demonstrate that various TLR agonists (TLR2, TLR9, TLR7-8) upregulate CD40, CD80, and CD86 expression on the surface of aged BMDCs (Fig. 1).

This observation is consistent with previous work showing that aging does not impair BMDCs' capacity to generate an immunological response to TLR activation [91].

Table 4 PCA for cytokines associated with T cell activation (CD4⁺ Tfh and CD8⁺ memory). Shown are PC score differences and Euclidean distance (in the space defined by PC1 and PC2) between treatments and control (untreated cells). We observed a cluster of adjuvants (NP + Mi + CpG, R848, NP + Mi + R848, CpG, MPLA, and LPS) that may have greater production of cytokines associated with T cell activation

Adjuvants	PC1(Adjuv)- PC1(Media)	PC2(Adjuv)- PC2(Media)	Distance(PC1,PC2)
Micelles	0.15	-0.46	0.48
FLA-BS	0.69	-0.48	0.84
CDN	0.99	0.47	1.09
MDP	1.12	-0.43	1.2
NP	1.2	-0.44	1.28
NP + Mi + CDN	2.5	2.53	3.55
NP + Mi + CpG	3.89	-0.06	3.89
R848	3.64	-1.48	3.93
NP + Mi + R848	3.84	-1.66	4.18
CpG	4.15	-0.69	4.21
MPLA	4.6	1.21	4.76
LPS	4.81	0.72	4.86

Table 5 PCA for proinflammatory cytokine secretion. Shown are PC score differences and Euclidean distance (in the space defined by PC1 and PC2) between treatments and control (untreated cells). We observed a cluster of adjuvants (NP + Mi + CpG, R848, MPLA, CpG, NP + Mi + R848, and LPS) that appear to be inducing the most proinflammatory cytokines

Adjuvants	PC1(Adjuv)- PC1(Media)	PC2(Adjuv)- PC2(Media)	Distance(PC1,PC2)
CDN	0.58	0	0.58
FLA-BS	1.27	-0.04	1.27
Micelles	1.33	0.45	1.4
MDP	1.58	-0.19	1.59
NP + Mi + CDN	1.7	0.76	1.86
NP	2.33	0.69	2.43
NP + Mi + CpG	3.64	-0.04	3.64
R848	4.56	-0.49	4.59
MPLA	4.69	0.46	4.71
CpG	4.88	-0.51	4.91
NP + Mi + R848	4.89	0.59	4.92
LPS	5.06	0.49	5.08

However, we found that FLA-BS (TLR 5 agonist) upregulated CD40 and CD80 but not CD86. Similarly, MDP, a ligand for the intracellular NOD2 receptor, upregulated both CD40 and CD80 but not CD86. Both flagellin and MDP have been shown to upregulate CD86 in human monocyte-derived DCs [92]; however, these studies

differed in either/both the cell type utilized or using cells from young adults. We have previously shown that NP activate BMDCs from young mice by increasing CD40, CD80, and CD86 expression [93]; however, we did not observe this effect in the current study with aged mice, though this may be, in part, due to differences in experimental design. In prior studies the cells were incubated for 48 h with NP, suggesting that NP may activate DC at a later time point. CDN, a stimulator of interferon genes (STING), only increased CD40 expression, but when combined with NP and Mi, showed a synergistic impact resulting in a substantial rise in CD80 and CD86 expression. Similarly, NP and Mi in combination with CpG (TLR 9) and R848 (TLR 7-8) significantly increased all cell surface markers.

The capacity of stimulants to increase aged BMDC immune effector functions was assessed by measuring cytokines linked with T cell activation and inflammation. The intensity and the direction of the immune response are determined by the processes through which certain stimulants exert their adjuvanticity. We found that LPS, MPLA, CpG, and R848 all generated high levels cytokines associated with T cell activation while simultaneously increasing levels of proinflammatory cytokines (Fig. 2). These findings align with previous work that suggests that TLR signals induce proinflammatory cytokines such as IL-1 β , TNF α and IL-12p40 [94]. FLA-BS and MDP had a modest effect on the production of cytokines but since they did not elicit the greatest response, they are not discussed in detail. Our results demonstrated that CDN-induced responses produced less inflammatory cytokines than the other TLR agonists, which is consistent with literature showing that CDN does not have the same inflammatory profile as other TLR agonists [95]. IFN- α and IFN- β assist in expanding antiviral pathways and play an important role in building adaptive immunity to viral infection by increasing T cell activation and survival [96]. Additionally, IFN- α and IFN- β have a crucial function in promoting DC responses [97, 98]. We assessed IFN α / β (Sup. Figure 2b) and found that CpG, LPS, and MPLA all substantially upregulated IFN α / β production. These findings are consistent with previous research showing that treatment with a TLR agonist results in an increase in the synthesis of IFN- α and IFN- β in mouse and human cells [99, 100]. On the other hand, both CDN and R848 increased IFN α but not IFN β . This result is consistent with earlier research, with one study reporting that TLR7/8 signaling increases IFN α [100]. However, when R848 and CDN were combined with Np and Mi, IFN- β production surged (Sup. Figure 2b). Similar results were obtained when combining NP and Mi with either CpG, CDN, or R848, on the secretion of various cytokines. While NP and Mi were not immunostimulatory on their

own, these data show that the biomaterials used in this study positively contribute to the generation of these vital cytokines (Signal 3) when combined with the appropriate adjuvants.

Through mixed linear model analysis, we obtained new semi-quantitative insights into how impactful the various adjuvant treatments were with respect to DC activation. However, we wanted to further understand the interplay between different adjuvants and combinations thereof with respect to their ability to stimulate costimulatory molecule expression and cytokine production. Therefore, we performed PCA and calculated PC scores between the various treatments and the control. These analyses allowed us to simultaneously analyze cytokines and costimulatory molecules in an effort to identify the “just right” combinations for adjuvants and nanoscale carriers (Figs. 3, 4 and 5 and Tables 2, 3, 4 and 5). These data show that while CpG has a propensity to substantially induce secretion of cytokines associated with T cell activation, it also induces higher proinflammatory cytokine production (Tables 4 and 5). On the other hand, cytokines associated with T cell activation were also enhanced by combining NP and Mi with CpG, without leading to excessive inflammation. This suggests that the inflammatory effects of CpG may be mitigated by formulating it with NP and Mi. Indeed, we have previously shown that the combination of CpG and NP offers robust and “universal” protection against influenza A virus when administered intranasally in young mice [47]. We also showed that while CDN is not highly inflammatory on its own, in combination with NP and Mi, the combination takes on a more proinflammatory profile and is more likely to be associated with cytokines that activate T cells (Tables 4 and 5). This observation is supported by our previous studies in which we showed that formulating CDN with nanovaccines protected both young and aged mice against influenza A infection [49].

The current studies offer a foundation to support the concept of judiciously combining adjuvants with nanoscale delivery platforms to induce a “just right” immune response in aged immune systems. We have shown that combining our nanoscale carriers with certain TLR and/or STING agonists can positively impact BMDCs generated from aged mice. We suggest that nanoparticles and micelles are working together in conjunction with these adjuvants to reduce the production of inflammatory cytokines while simultaneously boosting the production of T cell-related cytokines. Vaccines need to be developed that appropriately stimulate the aged immune system by balancing the induction of robust antibody and T cell responses with appropriately low levels of inflammation so as to not diminish the overall

immune response to vaccination. This balanced approach may be particularly important for mucosal vaccines delivered to sites of local inflammaging, such as the lung. In this context, combination approaches that formulate small molecule adjuvants with nanoparticles and micelles may provide a promising pathway forward to design next generation vaccines for older adults. While these results provide new insights into rational adjuvant selection and suggest that the combination of specific adjuvants and biomaterials provides enhanced immune activation while minimizing inflammation, caution should be used when inferring how these treatments may affect the immune system *in vivo*. We note that the *in vitro* experimental design used herein is a limitation to understanding responses at the level of the whole organism, but these studies provide a means for identifying combinations that show the most promise for future *in vivo* work.

Materials and methods

Study system

The effects of combinations of polymeric nanoparticles, micelles, and various small molecule agonists on the activation of bone marrow derived DCs (BMDCs) harvested from the femur and tibia of aged (≥ 20 months) C57BL/6 male mice ($n=6$) were studied. Bone marrow cells were cultured as outlined in Lutz et al. [101]. Briefly, cells were cultured in 10 mL RPMI 1640 medium supplemented with 100 U/mL penicillin, 100 mg/mL streptomycin, 2 mM glutamine, 10% FBS, and 20 ng/mL granulocyte-macrophage colony-stimulating factor (GM-CSF, Cat. #FB0875711Z, Peprotech, Rocky Hill, NJ) at approximately 5×10^6 cells per 100 mm plate. On day 3 of culture, 10 mL of medium containing GM-CSF was added. On days 6 and 8 of the culture period, approximately half of the total volume of medium was removed and replaced with freshly supplemented RPMI. On day 10 plates were gently rinsed to harvest non-adherent DCs for assessment of activation and costimulatory expression. Animals were obtained from Jackson Laboratory (Bar Harbor, ME) and maintained at Iowa State University following IACUC protocol #IACUC-20-199.

Stimulants

Polyanhydride NP synthesis

Polyanhydride monomers were synthesized using CPTEG and CPH as described previously [44, 45]. Using these monomers, a 20:80 CPTEG:CPH copolymer was synthesized by melt polycondensation as previously reported [45]. Using ^1H nuclear magnetic resonance spectroscopy (^1H NMR; DXR 500 Bruker, Billerica, MA) the final copolymer composition (23:77), molecular weight (11,000 g/mol), and purity were determined. Nanoparticles were synthesized using a solid-oil-oil double

emulsion technique as previously described [102]. In brief, a 20 mg mL⁻¹ solution of 20:80 CPTEG:CPH copolymer dissolved in methylene chloride was sonicated for 30 s to ensure complete dissolution of the polymer. The solution was then poured into chilled pentane (-10°C; 1:250 methylene chloride:pentane) and the resulting particles collected via vacuum filtration. Nanoparticle morphology and size (~200 nm) were verified with scanning electron microscopy (FEI Quanta 250, FEI, Hillsboro, OR).

PBC mi synthesis

The pentablock copolymer (PDEAEM-PEO-PPO-PEO-PDEAEM) was synthesized following our previously published protocol [46]. In short, atom transfer radical polymerization (ATRP) was used to synthesize the pentablock copolymer using a brominated Pluronic®-F127 as macroinitiator. The Pluronic F127 was dissolved in tetrahydrofuran and reacted overnight with triethylamine and 2-bromoisobutryl. To validate the end group functionalization, the product was precipitated in n-hexane and analyzed by ¹H NMR. The macroinitiator and DEAE monomer were then reacted by ATRP to synthesize the pentablock copolymer, with copper(I) oxide nanoparticles acting as the catalyst and N-propylpyridine methanamine acting as the complexing ligand [103]. The pentablock copolymer was characterized using ¹H NMR to determine purity and molecular weight (15,000 g/mol). The pentablock copolymer was dissolved in aqueous solution (12.5 µg/mL) to yield micelles.

Adjuvants

Lipopolysaccharide (LPS) (Cat. # L6529-1MG, Sigma Aldrich), Class B CpG oligonucleotide (CpG) (Cat.# tlr1-1668 InvivoGen), bis-(3'-5')-cyclic dimeric guanosine monophosphate (c-di-GMP) (CDN) (Cat.# tlr-nacdg, InvivoGen), muramyl dipeptide (MDP) (Cat.# tlrL-mdp InvivoGen), ultrapure flagellin from *B. subtilis* (FLSA-B) (Cat.# tlr1-pbsfla InvivoGen), monophosphoryl lipid A (MPLA) (Cat.# L6895 Sigma-Aldrich) and R848 (Cat.# tlr1-r848 InvivoGen) were purchased and used.

In vitro APC stimulation

BMDCs were seeded at 2.6 × 10⁵ cells per well in supplemented RPMI (as previously described) into 96-well round bottom tissue culture-treated microtiter plates (Cat. # FB0875711Z, Fisherbrand) at a volume of 200 µL per well. BMDCs were stimulated for 24 h with the adjuvants and concentrations shown in Table 1 as well as with double and triple combinations of adjuvants and biomaterials (e.g., NP + CpG, Mi + R848, NP + Mi + CpG, NP + Mi + CDN, NP + Mi + R848). Following stimulation, supernatants were collected and stored at -20°C

until use for quantification of cytokines. Cells were collected and assessed for surface marker expression.

Costimulatory molecule expression

Costimulatory molecule expression was assessed via flow cytometry. BMDCs were generated from the bone marrow of six aged mice across four separate days. Following culture, BMDCs were incubated with each treatment (i.e., single adjuvants, double, and triple combinations) for 24 h before assessment. Briefly, BMDCs (2.6 × 10⁵ per well in a 96-well plate) were stained with Zombie NIR dye (Cat. #423105, BioLegend), washed, then blocked with FcR blocking reagent (1 µL/well; 130-092-575 Miltenyi Biotech). Cells were then stained with anti-CD11c (BD Biosciences 557,401), anti-CD40 (BD Biosciences, 553,723), anti-CD80 (BD Biosciences, 560,526), and anti-CD86 antibodies (BD Biosciences, 560,581) by adding 0.25 µL/well of each monoclonal antibody. Following labeling, DCs were transferred to polystyrene tubes and fixed using BD stabilizing fixative (BD Bioscience, Franklin Lakes, NJ). Data were collected on a FACSCanto II flow cytometer (BD Bioscience, Franklin Lakes, NJ) and analyzed using FlowJo (FlowJo™ 10 LLC).

Cytokines

A total of 23 cytokines/chemokines were quantified using a multiplexed, bead-based immunoassay (Milliplex mouse cytokine/chemokine magnetic bead panel, Cat. # MCYTOMAG-70K, MTH17MAG-47K, and MECY2MAG-73K; Millipore, St Charles, MO) on a Luminex detection platform (Luminex, Austin, TX). All treatments (Table 1) were applied to cells from each of six mice and supernatants were collected from culture (*n* = 6 mice) following a 24 h incubation period. As cells were cultured on four separate days, supernatants were collected and stored at -20°C until use. Two panels of cytokines/chemokines were run using 25 µL supernatant per well, undiluted. For each plate, there were three biological replicates for each treatment. The second plate included an expanded panel of cytokines (see supplement Fig. S2b) and thus biological replicates for each cytokine/chemokine assayed ranged from *n* = 3 to 6. Assays were completed according to manufacturer protocol, with an overnight incubation (with agitation) at 4°C.

Statistical analyses

We performed a separate mixed linear model analysis for each dataset associated with costimulatory molecule expression and cytokine secretion. We also performed a mixed linear model analysis of the combined costimulatory molecule expression and cytokine secretion data. We present the results of these combined datasets in the manuscript and refer the reader to supplementary

materials for the analysis of separate datasets. For each separate costimulatory molecule expression and cytokine secretion dataset, we modelled the log of each measured response plus one (i.e., $\log(Y+1)$) as a function of adjuvant fixed effects, normally distributed mouse random effects, and normal random errors. For each of the combined analyses, we added fixed effects for plates to the mixed linear model. As part of each mixed linear model analysis, we performed individual tests on the regulation of each log-transformed response for each adjuvant/combination compared to unstimulated cells. Specifically, we tested the difference between the linear coefficients of each adjuvant and the unstimulated cells. Furthermore, we use adjusted p -values, referred to as q -values, to control false discovery rate control (FDR) for the collection of tests within each dataset [104]. The procedure was implemented in R using the functions “lme4::lmer”, “lmerTest::contest” [105], “stats::p.adjust”, and “ComplexHeatmap::Heatmap” [106].

Additionally, we performed principal component analysis (PCA) to gain insights into clustering effects of single adjuvants and treatment combinations on the regulation of both costimulatory expression and cytokine production. Responses to treatment were log-transformed ($\log(Y+1)$) and standardized. As a means of facilitating the clustering, all treatment groups were compared to untreated cells. The numbers of clusters were selected by the silhouette method [107], followed by the identification of clusters with the k-means clustering method [108]. The procedure was implemented in R using the functions “stats::prcomp”, “factoextra::fviz_nbclust”, “stats::kmeans”, and “factoextra::fviz_cluster” [109].

Supplementary Information

The online version contains supplementary material available at <https://doi.org/10.1186/s12979-023-00332-0>.

Additional file 1: Fig. S1. Estimates of \log_2 fold change (\log_2FC) and regulation tests for costimulatory molecules expressed on CD11c⁺ cell surfaces after stimulation by single adjuvant, dual treatments, and controls. Color scale represents the estimated \log_2 fold change (\log_2FC) in molecule expression to a specific treatment relative to untreated cells. Asterisks represent the degree of significance for a given treatment relative to untreated cells: **** $q < 0.001$, *** $q < 0.01$, ** $q < 0.05$. Responses to treatments were measured for each of six mice ($n=6$) with multiple replicates. **Fig. S2.** a. Estimates of \log_2 fold change (\log_2FC) and tests of regulation from mixed linear model analysis of cytokines. This panel includes single adjuvants and their related double, and triple combinations. The color scale represents the estimated \log_2 fold change (\log_2FC) of a given cytokine to a specific treatment relative to untreated cells. Asterisks represent the degree of significance for each treatment relative to untreated cells: **** $q < 0.001$, *** $q < 0.01$, ** $q < 0.05$. Each treatment was tested on cells harvested from each of $n=3-6$ animals. b. Estimates of \log_2 fold change (\log_2FC) and tests of regulation from mixed linear model analysis of an expanded panel of cytokines. The color scale represents the estimated \log_2 fold change (\log_2FC) of a given cytokine to a specific treatment relative to untreated cells. Asterisks represent the degree of significance for each treatment relative to untreated cells: **** $q < 0.001$, *** $q < 0.01$,

** $q < 0.05$. Each treatment was tested on cells harvested from each of $n=3$ animals on a single kit. **Fig. S3.** Pictorial representation of the data in Table 2. We observed a cluster of treatments (cluster 2, comprised of MPLA, LPS, CpG, and NP + Mi + CpG) that suggest a greater upregulation in costimulatory molecule expression than the other adjuvants. **Fig. S4.** Pictorial representation of the data in Table 3. We observed a cluster of treatments (cluster 1, comprised of NP + Mi + CpG, R848, MPLA, CpG, LPS, and NP + R848 + Mi) that suggests a stronger upregulation of cytokine secretion than the other adjuvants shown in cluster 2. **Fig. S5.** Pictorial representation of the data in Table 4. Cluster 1 (NP + Mi + CpG, R848, NP + Mi + R848, CpG, MPLA, and LPS) contains treatments which are most strongly associated with T cell activation. **Fig. S6.** Pictorial representation of the data in Table 5. Cluster 2 (NP + Mi + CpG, MPLA, CpG, NP + Mi + R848, LPS, and R848) contains treatments most strongly associated with proinflammatory cytokine secretion.

Acknowledgments

The authors acknowledge support from the Iowa State University Nanovaccine Institute. B.N is grateful to the Vlasta Klima Balloun Faculty Chair and S.K.M. is grateful to the Carol Vohs Johnson Chair.

Authors' contributions

AA, KGH, SKM, MJW, MLK, and BN conceptualized the study design and methodology. MLK, SKM, and BN supervised all work; MLK and BN obtained funding. AA and KGH carried out all experiments. ZG and DN performed statistical analyses. AA, KGH, MLK, and BN drafted the manuscript. All authors contributed to the final manuscript. The author(s) read and approved the final manuscript.

Funding

The authors acknowledge financial support from NIH-NIAID (R01 AI141196 and R01 AI154458).

Availability of data and materials

The datasets used and/or analyzed during the current study are available from the corresponding author on reasonable request.

Declarations

Ethics approval and consent to participate

All procedures involving animals were approved by the Institutional Animal Care and Use Committee at Iowa State University under protocol #IACUC-20-199.

Consent for publication

Not applicable.

Competing interests

Balaji Narasimhan and Michael Wannemuehler are co-founders of ImmunoNanoMed Inc., a start-up with business interests in the development of nano-based vaccines against infectious diseases. Narasimhan also has a financial interest in Degimflex LLC. Surya Mallapragada is a co-founder of Degimflex LLC, a start-up with business interests in the development of flexible degradable electronic films for biomedical applications. She also has a financial interest in ImmunoNanoMed Inc.

Author details

¹Nanovaccine Institute, Iowa State University, Ames, IA 50011, USA. ²Department of Chemical and Biological Engineering, Iowa State University, Ames, IA 50011, USA. ³Department of Statistics, Iowa State University, Ames, IA 50011, USA. ⁴Department of Kinesiology, Iowa State University, Ames, IA 50011, USA.

Received: 11 October 2022 Accepted: 5 February 2023

Published online: 09 March 2023

References

- Montecino-Rodriguez E, Berent-Maoz B, Dorshkind K. Causes, consequences, and reversal of immune system aging. *J Clin Invest*. 2013;123(3):958–65.
- Crooke SN, Ovsyannikova IG, Poland GA, Kennedy RB. Immunosenescence: a systems-level overview of immune cell biology and strategies for improving vaccine responses. *Exp Gerontol*. 2019;124:110632.
- Santoro A, Bientinesi E, Monti D. Immunosenescence and inflammaging in the aging process: age-related diseases or longevity? *Ageing Res Rev*. 2021;71:101422.
- Salminen A. Immunosuppressive network promotes immunosenescence associated with aging and chronic inflammatory conditions. *J Mol Med (Berl)*. 2021;99(11):1553–69.
- Lee KA, Flores RR, Jang IH, Saathoff A, Robbins PD. Immune senescence, immunosenescence and aging. *Front Aging*. 2022;3:900028.
- Balistreri CR, Candore G, Accardi G, Colonna-Romanò G, Lio D. NF- κ B pathway activators as potential ageing biomarkers: targets for new therapeutic strategies. *Immun Ageing*. 2013;10(1):1–16.
- Franceschi C, Bonafe M, Valensin S, Olivieri F, De Luca M, Ottaviani E, et al. Inflamm-aging. An evolutionary perspective on immunosenescence. *Ann N Y Acad Sci*. 2000;908(1):244–54.
- Franceschi C, Garagnani P, Vitale G, Capri M, Salvioli S. Inflammaging and 'Garb-aging'. *Trends Endocrinol Metab*. 2017;28(3):199–212.
- Campbell RA, Docherty MH, Ferenbach DA, Mylonas KJ. The role of ageing and parenchymal senescence on macrophage function and fibrosis. *Front Immunol*. 2021;12:700790.
- De Maeyer RPH, Chambers ES. The impact of ageing on monocytes and macrophages. *Immunol Lett*. 2021;230:1–10.
- Le Lee J, Linterman MA. Mechanisms underpinning poor antibody responses to vaccines in ageing. *Immunol Lett*. 2022;241:1–14.
- Baylis D, Bartlett DB, Patel HP, Roberts HC. Understanding how we age: insights into inflammaging. *Longev Healthspan*. 2013;2(1):8.
- Metcalf TU, Cubas RA, Gheime K, Cartwright MJ, Grevenynghe JV, Richner JM, et al. Global analyses revealed age-related alterations in innate immune responses after stimulation of pathogen recognition receptors. *Ageing Cell*. 2015;14(3):421–32.
- Panda A, Qian F, Mohanty S, van Duin D, Newman FK, Zhang L, et al. Age-associated decrease in TLR function in primary human dendritic cells predicts influenza vaccine response. *J Immunol*. 2010;184(5):2518–27.
- Medvedev AE, Sabroe I, Hasday JD, Vogel SN. Invited review: tolerance to microbial TLR ligands: molecular mechanisms and relevance to disease. *J Endotoxin Res*. 2006;12(3):133–50.
- Chen JQ, Szodoray P, Zeher M. Toll-like receptor pathways in autoimmune diseases. *Clin Rev Allergy Immunol*. 2016;50(1):1–17.
- Dudani R, Chapdelaine Y, van Faassen H, Smith DK, Shen H, Krishnan L, et al. Preexisting inflammation due to *Mycobacterium bovis* BCG infection differentially modulates T-cell priming against a replicating or nonreplicating immunogen. *Infect Immun*. 2002;70(4):1957–64.
- Macri C, Dumont C, Johnston AP, Mintern JD. Targeting dendritic cells: a promising strategy to improve vaccine effectiveness. *Clin Transl Immunol*. 2016;5(3):e66.
- Akira S, Uematsu S, Takeuchi O. Pathogen recognition and innate immunity. *Cell*. 2006;124(4):783–801.
- Medzhitov R, Janeway CA Jr. Decoding the patterns of self and non-self by the innate immune system. *Science*. 2002;296(5566):298–300.
- Martinon F, Tschopp J. NLRs join TLRs as innate sensors of pathogens. *Trends Immunol*. 2005;26(8):447–54.
- Shaw PJ, Lamkanfi M, Kanneganti TD. NOD-like receptor (NLR) signaling beyond the inflammasome. *Eur J Immunol*. 2010;40(3):624–7.
- Figdor CG, van Kooyk Y, Adema GJ. C-type lectin receptors on dendritic cells and Langerhans cells. *Nat Rev Immunol*. 2002;2(2):77–84.
- Geijtenbeek TB, van Vliet SJ, Engering A, t Hart BA, van Kooyk Y. Self- and nonself-recognition by C-type lectins on dendritic cells. *Annu Rev Immunol*. 2004;22:33–54.
- Iwasaki A, Medzhitov R. Toll-like receptor control of the adaptive immune responses. *Nat Immunol*. 2004;5(10):987–95.
- Lee HK, Iwasaki A. Innate control of adaptive immunity: dendritic cells and beyond. *Semin Immunol*. 2007;19:48–55.
- Connors J, Bell MR, Marcy J, Kutzler M, Haddad EK. The impact of immuno-aging on SARS-CoV-2 vaccine development. *Geroscience*. 2021;43(1):31–51.
- Stebegg M, Bignon A, Hill DL, Silva-Cayetano A, Krueger C, Vanderleyden I, et al. Rejuvenating conventional dendritic cells and T follicular helper cell formation after vaccination. *Elife*. 2020;9:e52473.
- Lefebvre JS, Maue AC, Eaton SM, Lanthier PA, Tighe M, Haynes L. The aged microenvironment contributes to the age-related functional defects of CD4 T cells in mice. *Ageing Cell*. 2012;11(5):732–40.
- Brahmakshatriya V, Kuang Y, Devarajan P, Xia J, Zhang W, Vong AM, et al. IL-6 production by TLR-activated APC broadly enhances aged cognate CD4 helper and B cell antibody responses in vivo. *J Immunol*. 2017;198(7):2819–33.
- Gupta S. Role of dendritic cells in innate and adaptive immune response in human aging. *Exp Gerontol*. 2014;49:47–52.
- Borges RC, Hohmann MS, Borghi SM. Dendritic cells in COVID-19 immunopathogenesis: insights for a possible role in determining disease outcome. *Int Rev Immunol*. 2021;40(1–2):108–25.
- Agrawal A, Agrawal S, Gupta S. Dendritic cells in human aging. *Exp Gerontol*. 2007;42(5):421–6.
- Perez CR, De Palma M. Engineering dendritic cell vaccines to improve cancer immunotherapy. *Nat Commun*. 2019;10(1):5408.
- Alter G, Sekaly RP. Beyond adjuvants: antagonizing inflammation to enhance vaccine immunity. *Vaccine*. 2015;33(Suppl 2):B55–9.
- Pulendran B, S. Arunachalam P, O'Hagan DT. Emerging concepts in the science of vaccine adjuvants. *Nat Rev Drug Discov*. 2021;20(6):454–75.
- Kovacs EJ, Boe DM, Boule LA, Curtis BJ. Inflammaging and the lung. *Clin Geriatr Med*. 2017;33(4):459–71.
- Frasca D, Blomberg BB. Inflammaging decreases adaptive and innate immune responses in mice and humans. *Biogerontology*. 2016;17(1):7–19.
- Reed SG, Orr MT, Fox CB. Key roles of adjuvants in modern vaccines. *Nat Med*. 2013;19(12):1597–608.
- Wu TYH, Singh M, Miller AT, De Gregorio E, Doro F, D'Oro U, et al. Rational design of small molecules as vaccine adjuvants. *Sci Transl Med*. 2014;6(263):263ra160–263ra160.
- Pereira B, Xu XN, Akbar AN. Targeting inflammation and immunosenescence to improve vaccine responses in the elderly. *Front Immunol*. 2020;11:583019.
- Mallapragada SK, Narasimhan B. Immunomodulatory biomaterials. *Int J Pharm*. 2008;364(2):265–71.
- Brem H, Kader A, Epstein JI, Tamargo RJ, Domb A, Langer R, et al. Biocompatibility of a biodegradable, controlled-release polymer in the rabbit brain. *Sel Cancer Ther*. 1989;5(2):55–65.
- Conix A. Poly [1, 3-bis (p-carboxyphenoxy)-propane anhydride]. *Macromol Synth*. 1966;2(1):95–6.
- Torres MP, Vogel BM, Narasimhan B, Mallapragada SK. Synthesis and characterization of novel polyanhydrides with tailored erosion mechanisms. *J Biomed Mater Res A*. 2006;76(1):102–10.
- Determan MD, Cox JP, Seifert S, Thiagarajan P, Mallapragada SK. Synthesis and characterization of temperature and pH-responsive pentablock copolymers. *Polymer*. 2005;46(18):6933–46.
- Zacharias ZR, Ross KA, Hornick EE, Goodman JT, Narasimhan B, Waldschmidt TJ, et al. Polyanhydride Nanovaccine induces robust pulmonary B and T cell immunity and confers protection against homologous and heterologous influenza virus infections. *Front Immunol*. 2018;9:1953.
- Senapati S, Darling RJ, Ross KA, Wannemuehler MJ, Narasimhan B, Mallapragada SK. Self-assembling synthetic nanoadjuvant scaffolds cross-link B cell receptors and represent new platform technology for therapeutic antibody production. *Sci Adv*. 2021;7(32):eabj1691.
- Ross K, Senapati S, Alley J, Darling R, Goodman J, Jefferson M, et al. Single dose combination nanovaccine provides protection against influenza A virus in young and aged mice. *Biomater Sci*. 2019;7(3):809–21.
- Shakya AK, Nandakumar KS. Applications of polymeric adjuvants in studying autoimmune responses and vaccination against infectious diseases. *J R Soc Interface*. 2013;10(79):20120536.
- Brem H, Domb A, Lenartz D, Dureza C, Olivi A, Epstein JI. Brain biocompatibility of a biodegradable controlled release polymer consisting of anhydride copolymer of fatty-acid dimer and Sebacic acid. *J Control Release*. 1992;19(1–3):325–9.

52. Huntimer L, Ramer-Tait AE, Petersen LK, Ross KA, Walz KA, Wang C, et al. Evaluation of biocompatibility and administration site reactogenicity of polyanhydride-particle-based platform for vaccine delivery. *Adv Healthc Mater.* 2013;2(2):369–78.
53. Adams JR, Goswami M, Pohl NLB, Mallapragada SK. Synthesis and functionalization of virus-mimicking cationic block copolymers with pathogen-associated carbohydrates as potential vaccine adjuvants. *RSC Adv.* 2014;4(30):15655–63.
54. Agarwal A, Mallapragada SK. Synthetic sustained gene delivery systems. *Curr Top Med Chem.* 2008;8(4):311–30.
55. Determan MD, Cox JP, Mallapragada SK. Drug release from pH-responsive thermogelling pentablock copolymers. *J Biomed Mater Res A.* 2007;81(2):326–33.
56. Zhang B, Jia F, Fleming MQ, Mallapragada SK. Injectable self-assembled block copolymers for sustained gene and drug co-delivery: an in vitro study. *Int J Pharm.* 2012;427(1):88–96.
57. Zhang B, Kanapathipillai M, Bisso P, Mallapragada S. Novel pentablock copolymers for selective gene delivery to cancer cells. *Pharm Res.* 2009;26(3):700–13.
58. Kabanov AV, Lemieux P, Vinogradov S, Alakhov V. Pluronic block copolymers: novel functional molecules for gene therapy. *Adv Drug Deliv Rev.* 2002;54(2):223–33.
59. Kreuter J, Liehl E, Berg U, Soliva M, Speiser PP. Influence of hydrophobicity on the adjuvant effect of particulate polymeric adjuvants. *Vaccine.* 1988;6(3):253–6.
60. Wenzel JG, Balaji KS, Koushik K, Navarre C, Duran SH, Rahe CH, et al. Pluronic F127 gel formulations of deslorelin and GnRH reduce drug degradation and sustain drug release and effect in cattle. *J Control Release.* 2002;85(1-3):51–9.
61. Kohli AK, Alpar HO. Potential use of nanoparticles for transcutaneous vaccine delivery: effect of particle size and charge. *Int J Pharm.* 2004;275(1-2):13–7.
62. Slutter B, Plapied L, Fievez V, Sande MA, des Rieux A, Schneider YJ, et al. Mechanistic study of the adjuvant effect of biodegradable nanoparticles in mucosal vaccination. *J Control Release.* 2009;138(2):113–21.
63. Rothenfusser S, Hornung V, Ayyoub M, Britsch S, Towarowski A, Krug A, et al. CpG-A and CpG-B oligonucleotides differentially enhance human peptide-specific primary and memory CD8+ T-cell responses in vitro. *Blood.* 2004;103(6):2162–9.
64. Krieg AM. CpG motifs in bacterial DNA and their immune effects. *Annu Rev Immunol.* 2002;20(1):709–60.
65. Verthelyi D, Ishii KJ, Gursel M, Takeshita F, Klinman DM. Human peripheral blood cells differentially recognize and respond to two distinct CPG motifs. *J Immunol.* 2001;166(4):2372–7.
66. Hanagata N. Structure-dependent immunostimulatory effect of CpG oligodeoxynucleotides and their delivery system. *Int J Nanomedicine.* 2012;7:2181–95.
67. Karaolis DKR, Means TK, Yang D, Takahashi M, Yoshimura T, Muraile E, et al. Bacterial c-di-GMP is an immunostimulatory molecule. *J Immunol.* 2007;178(4):2171–81.
68. Hayashi F, Smith KD, Ozinsky A, Hawn TR, Yi EC, Goodlett DR, et al. The innate immune response to bacterial flagellin is mediated by Toll-like receptor 5. *Nature.* 2001;410(6832):1099–103.
69. Zhao Y, Yang J, Shi J, Gong YN, Lu Q, Xu H, et al. The NLR4 inflammasome receptors for bacterial flagellin and type III secretion apparatus. *Nature.* 2011;477(7366):596–600.
70. Mizel SB, Honko AN, Moors MA, Smith PS, West AP. Induction of macrophage nitric oxide production by gram-negative flagellin involves signaling via heteromeric toll-like receptor 5/toll-like receptor 4 complexes. *J Immunol.* 2003;170(12):6217–23.
71. Buzzo CL, Campopiano JC, Massis LM, Lage SL, Cassado AA, Leme-Souza R, et al. A novel pathway for inducible nitric-oxide synthase activation through inflammasomes. *J Biol Chem.* 2010;285(42):32087–95.
72. Matusiak M, Van Opendenbosch N, Vande Walle L, Sirard JC, Kanneganti TD, Lamkanfi M. Flagellin-induced NLR4 phosphorylation primes the inflammasome for activation by NAIP5. *Proc Natl Acad Sci U S A.* 2015;112(5):1541–6.
73. Thompson BS, Chilton PM, Ward JR, Evans JT, Mitchell TC. The low-toxicity versions of LPS, MPL adjuvant and RC529, are efficient adjuvants for CD4+ T cells. *J Leukoc Biol.* 2005;78(6):1273–80.
74. Fransen F, Boog CJ, van Putten JP, van der Ley P. Agonists of Toll-like receptors 3, 4, 7, and 9 are candidates for use as adjuvants in an outer membrane vaccine against *Neisseria meningitidis* serogroup B. *Infect Immun.* 2007;75(12):5939–46.
75. Evans JT, Cluff CW, Johnson DA, Lacy MJ, Persing DH, Baldrige JR. Enhancement of antigen-specific immunity via the TLR4 ligands MPL adjuvant and Ribi.529. *Expert Rev Vaccines.* 2003;2(2):219–29.
76. Moreira LO, El Kasmi KC, Smith AM, Finkelstein D, Fillon S, Kim YG, et al. The TLR2-MyD88-NOD2-RIPK2 signalling axis regulates a balanced pro-inflammatory and IL-10-mediated anti-inflammatory cytokine response to gram-positive cell walls. *Cell Microbiol.* 2008;10(10):2067–77.
77. Hsu LC, Ali SR, McGillivray S, Tseng PH, Mariathasan S, Humke EW, et al. A NOD2-NALP1 complex mediates caspase-1-dependent IL-1 β secretion in response to bacillus anthracis infection and muramyl dipeptide. *Proc Natl Acad Sci U S A.* 2008;105(22):7803–8.
78. Kim HJ, Yang JS, Woo SS, Kim SK, Yun CH, Kim KK, et al. Lipoteichoic acid and muramyl dipeptide synergistically induce maturation of human dendritic cells and concurrent expression of proinflammatory cytokines. *J Leukoc Biol.* 2007;81(4):983–9.
79. Vasilakos JP, Smith RM, Gibson SJ, Lindh JM, Pederson LK, Reiter MJ, et al. Adjuvant activities of immune response modifier R-848: comparison with CpG ODN. *Cell Immunol.* 2000;204(1):64–74.
80. Petersen LK, Xue L, Wannemuehler MJ, Rajan K, Narasimhan B. The simultaneous effect of polymer chemistry and device geometry on the in vitro activation of murine dendritic cells. *Biomaterials.* 2009;30(28):5131–42.
81. Goodman JT, Ramirez JEV, Boggiatto PM, Roychoudhury R, Pohl NLB, Wannemuehler MJ, et al. Nanoparticle chemistry and functionalization differentially regulates dendritic cell-nanoparticle interactions and triggers dendritic cell maturation. *Part Part Syst Charact.* 2014;31(12):1269–80.
82. Senapati S, Darling RJ, Loh D, Schneider IC, Wannemuehler MJ, Narasimhan B, et al. Pentablock copolymer micelle nanoadjuvants enhance cytosolic delivery of antigen and improve vaccine efficacy while inducing low inflammation. *ACS Biomater Sci Eng.* 2019;5(3):1332–42.
83. Agrawal A, Agrawal S, Cao JN, Su H, Osann K, Gupta S. Altered innate immune functioning of dendritic cells in elderly humans: a role of phosphoinositide 3-kinase-signaling pathway. *J Immunol.* 2007;178(11):6912–22.
84. Lord JM. The effect of aging of the immune system on vaccination responses. *Hum Vaccin Immunother.* 2013;9(6):1364–7.
85. Hainz U, Jenewein B, Asch E, Pfeiffer KP, Berger P, Grubeck-Loebenstien B. Insufficient protection for healthy elderly adults by tetanus and TBE vaccines. *Vaccine.* 2005;23(25):3232–5.
86. Coe CL, Lubach GR, Kinnard J. Immune senescence in old and very old rhesus monkeys: reduced antibody response to influenza vaccination. *Age.* 2012;34(5):1169–77.
87. Steinman RM, Banchereau J. Taking dendritic cells into medicine. *Nature.* 2007;449(7161):419–26.
88. Hackstein H, Thomson AW. Dendritic cells: emerging pharmacological targets of immunosuppressive drugs. *Nat Rev Immunol.* 2004;4(1):24–34.
89. Coffman RL, Sher A, Seder RA. Vaccine adjuvants: putting innate immunity to work. *Immunity.* 2010;33(4):492–503.
90. Brito LA, O'Hagan DT. Designing and building the next generation of improved vaccine adjuvants. *J Control Release.* 2014;190:563–79.
91. Tesar BM, Walker WE, Unternaehrer J, Joshi NS, Chandele A, Haynes L, et al. Nurine myeloid dendritic cell-dependent toll-like receptor immunity is preserved with aging. *Aging Cell.* 2006;5(6):473–86.
92. Fujimura T, Yamasaki K, Hidaka T, Ito Y, Aiba S. A synthetic NOD2 agonist, muramyl dipeptide (MDP)-Lys (L18) and IFN-beta synergistically induce dendritic cell maturation with augmented IL-12 production and suppress melanoma growth. *J Dermatol Sci.* 2011;62(2):107–15.
93. Darling R, Senapati S, Christiansen J, Liu L, Ramer-Tait AE, Narasimhan B, et al. Polyanhydride nanoparticles induce low inflammatory dendritic cell activation resulting in CD8+ T cell memory and delayed tumor progression. *Int J Nanomedicine.* 2020;15:6579–92.
94. Ozato K, Tsujimura H, Tamura T. Toll-like receptor signaling and regulation of cytokine gene expression in the immune system. *BioTechniques.* 2002;33(45):66–68 70, 72.

95. Darling RJ, Senapati S, Kelly SM, Kohut ML, Narasimhan B, Wannemuehler MJ. STING pathway stimulation results in a differentially activated innate immune phenotype associated with low nitric oxide and enhanced antibody titers in young and aged mice. *Vaccine*. 2019;37(20):2721–30.
96. Biron CA. Role of early cytokines, including alpha and beta interferons (IFN- α/β), in innate and adaptive immune responses to viral infections. *Semin Immunol*. 1998;10:383–90.
97. Tough DF. Type I interferon as a link between innate and adaptive immunity through dendritic cell stimulation. *Leuk Lymphoma*. 2004;45(2):257–64.
98. Montoya M, Schiavoni G, Mattei F, Gresser I, Belardelli F, Borrow P, et al. Type I interferons produced by dendritic cells promote their phenotypic and functional activation. *Blood*. 2002;99(9):3263–71.
99. Le Bon A, Tough DF. Links between innate and adaptive immunity via type I interferon. *Curr Opin Immunol*. 2002;14(4):432–6.
100. Honda K, Yanai H, Mizutani T, Negishi H, Shimada N, Suzuki N, et al. Role of a transductional-transcriptional processor complex involving MyD88 and IRF-7 in Toll-like receptor signaling. *Proc Natl Acad Sci U S A*. 2004;101(43):15416–21.
101. Lutz MB, Kükutsch N, Ogilvie AL, Rossner S, Koch F, Romani N, et al. An advanced culture method for generating large quantities of highly pure dendritic cells from mouse bone marrow. *J Immunol Methods*. 1999;223(1):77–92.
102. Ulery BD, Phanse Y, Sinha A, Wannemuehler MJ, Narasimhan B, Bellaire BH. Polymer chemistry influences monocytic uptake of polyanhydride nanospheres. *Pharm Res*. 2009;26(3):683–90.
103. Adams JR, Mallapragada SK. Novel atom transfer radical polymerization method to yield copper-free block Copolymeric biomaterials. *Macromol Chem Phys*. 2013;214(12):1321–5.
104. Benjamini Y, Hochberg Y. Controlling the false discovery rate - a practical and powerful approach to multiple testing. *J R Stat Soc Ser B Stat Methodol*. 1995;57(1):289–300.
105. Bates D, Mächler M, Bolker B, Walker S. Fitting linear mixed-effects models using lme4. *arXiv preprint arXiv:1406.5823*; 2014.
106. Gu Z. Complex heatmap visualization. *iMeta*. 2022;1(3):e43.
107. Rousseeuw PJ. Silhouettes - a graphical aid to the interpretation and validation of cluster-analysis. *J Comput Appl Math*. 1987;20(20):53–65.
108. Hartigan JA, Wong MA. Algorithm AS 136: A K-means Clustering Algorithm. *J R Stat Soc Ser C Appl Stat*. 1979;28:100–8.
109. Kassambara A, Mundt F. "Package 'factoextra'." Extract and visualize the results of multivariate data analyses. R package version 1.0.7. 2020. <https://CRAN.R-project.org/package=factoextra>.

Publisher's Note

Springer Nature remains neutral with regard to jurisdictional claims in published maps and institutional affiliations.

Ready to submit your research? Choose BMC and benefit from:

- fast, convenient online submission
- thorough peer review by experienced researchers in your field
- rapid publication on acceptance
- support for research data, including large and complex data types
- gold Open Access which fosters wider collaboration and increased citations
- maximum visibility for your research: over 100M website views per year

At BMC, research is always in progress.

Learn more biomedcentral.com/submissions

